JOURNAL OF MATERIALS SCIENCE 11 (1976) 134–141

Low field anomalies in the magnetization behaviour of superconducting Zr-Nb alloys

S. L. NARASIMHAN, R. TAGGART, D. H. POLONIS
College of Engineering, FB-10, University of Washington, Seattle, Washington, USA

The magnetization behaviour of superconducting Zr–Nb alloys has been examined to determine the effects of constitution and microstructure on anomalies in the form of a "peak effect" and flux instabilities. It is concluded that both of these phenomena depend on the particle size, volume fraction, and distribution of the omega phase. The occurrence of both anomalies is explained in terms of the transition of the omega phase from the superconducting to normal state as the applied field is increased. The absence of anomalies in reverted and re-aged alloys reflects the predominant role of the solute lean zones in determining the bulk superconducting properties.

1. Introduction

In a two-phase alloy where a superconducting matrix contains dispersed particles, strong proximity effects arise when the particle size approaches the coherence length of the alloy [1–3]. Screening effects are observed when a superconducting matrix phase forms a continuous film that shields a dispersed phase from the externally applied field. Both the proximity and screening effects assume an important role in determining the bulk superconducting properties of multiphase alloys and composite films [1].

Beta stabilized Zr–Nb alloys aged at 350° C exhibit a strong proximity effect between the beta matrix and the omega particles precipitated during ageing. As a result of this proximity effect the bulk superconducting transition temperature of the Zr–Nb alloys is lowered, and a double transition is detected in zero magnetic field [4]. Multiple ageing and reversion treatments have been used in the present study to modify the microstructure and constitution of Zr–Nb alloys. The influence of the microstructural and constitutional changes on the proximity and screening effects has been examined by means of magnetization measurements carried out in a persistent magnetic field.

2. Experimental procedures

Zr–Nb alloys containing 15 and 20 at. % Nb were prepared by a standard levitation melting technique employing an atmosphere of purified helium. The alloy constituents were 99.95% pure Zr and 99.8% pure Nb. On the basis of the weight loss incurred during melting, the errors in alloy composition were estimated to be no greater than 0.1%. The alloys were cast in the form of cylindrical ingots 3.5 mm diameter and approximately 4 cm long; then they were wrapped in pure Ta foil, sealed in Vycor capsules under a vacuum of 10^{-6} Torr and homogenized at 1000° C for 3 days. After the heat-treatment, the homogeneity was verified by electron microprobe analysis. The specimens prepared from the ingots were wrapped in Ta foil and solution-treated at 1050° C for 1 h in an atmosphere of high purity helium, after which they were quenched into water at room temperature.

The magnetization measurements on the heat-treated specimens were carried out in a highly stable persistent magnetic field of homogeneity better than 0.1% over the distance traversed by the specimen. A ballistic technique described in a previous paper [5] was employed to determine the isothermal magnetization characteristics. The data were analysed by the CDC 6400 computer, and the results were plotted directly by a Calcomp plotter.

3. Experimental results

3.1. Magnetization behaviour

The magnetization behaviour of a quenched Zr–15 at. % Nb alloy at 4.2 K is represented by curve A

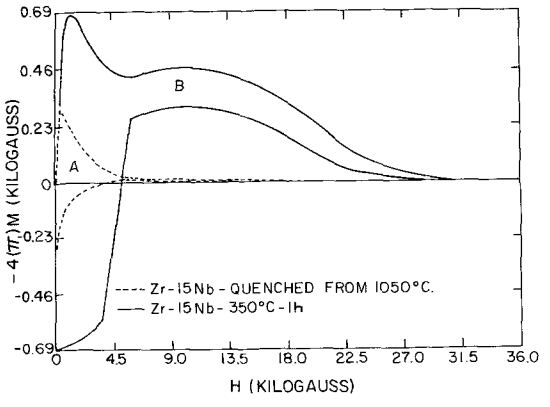

Figure 1 The isothermal magnetization behaviour at 4.2 K, of a Zr–15 at.% Nb alloy, (A) quenched from 1050° C, (B) quenched and aged at 350° C for 1 h, showing the peak effect.

in Fig. 1, and the magnetization curve obtained at 4.2 K for the same alloy, aged at 350° C for 1 h is shown as curve B in Fig. 1. A second peak occurs in curve B at an applied field of approximately 10 kG and is reversible, as shown in Fig. 1. Chemically etching the specimen or light mechanical grinding with abundant cooling demonstrated that the peak effect was independent of surface characteristics. The appearance of a second peak in the magnetization behaviour is consistent with the double superconducting transition that is observed in the inductance–temperature curve reported for the same alloy under identical conditions of thermal treatment [4]. A similar but more pronounced second peak in the magnetization behaviour occurs at an applied field of about 6 kG as shown in curve A of Fig. 2 for a double ageing treatment which consisted of 25 h at 225° C and 12 h at 350° C.

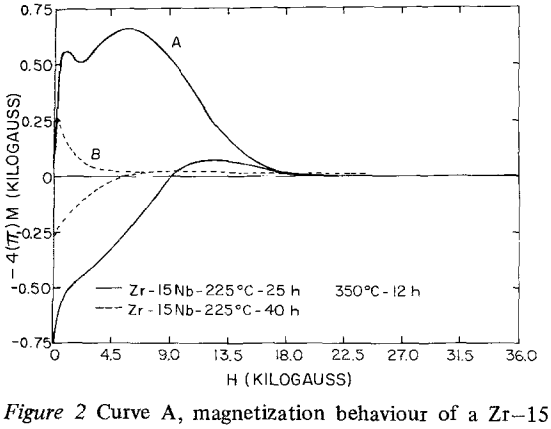

Figure 2 Curve A, magnetization behaviour of a Zr–15 at.% Nb alloy, first aged at 225° C for 25 h and subsequently aged at 350° C for 12 h, showing the peak effect. Curve B, the magnetization behaviour of a Zr–15 at.% Nb alloy aged for 40 h at 225° C. No peak effect is observed.

Ageing the quenched alloy of 225° C for 40 h produced little change in the irreversible magnetization behaviour, except for an increase in the value of H_{c2} from approximately 20 to 25 kG, as shown by curve B in Fig. 2. A second ageing treatment at 350° C for 6 h following the one at 225° C for 40 h, resulted in the development of a pronounced second peak in the magnetization curve at a magnetic field value of about 8 kG and a decrease in the value of H_{c2} to about 16 kG, as shown in Fig. 3. The peak was reproducible and did not depend on the surface condition of the sample; it could be eliminated by a reversion treatment at 500° C for 1 min as shown in Fig. 4, and the value of H_{c2} increases to about 32 kG. Prolonged ageing of the quenched alloy resulted in a flux jump at approximately 4 kG rather than the peak effect, as shown in Fig. 5 for an alloy aged 24 h at 350° C.

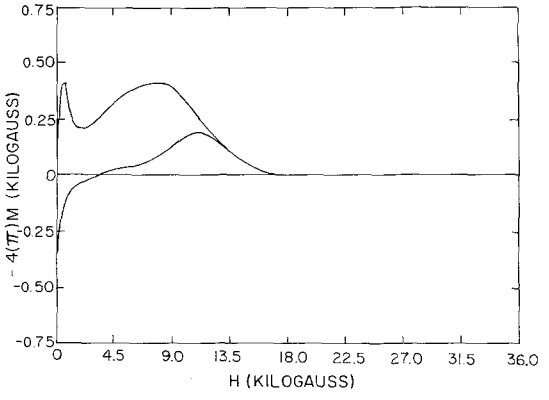

Figure 3 The second peak in the magnetization established by a double ageing treatment at 350° C for 6 h following an ageing treatment at 225° C for 40 h, for a Zr–15 at.% Nb alloy.

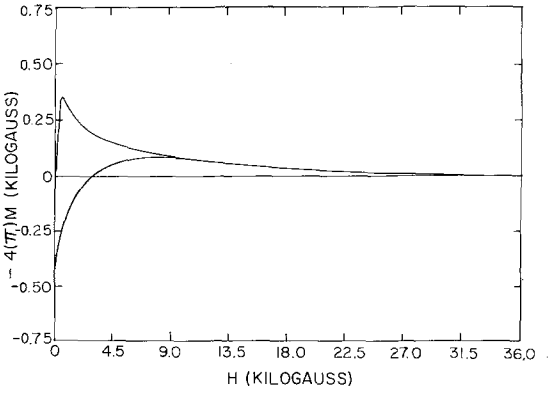

Figure 4 The effect of reversion at 550° C for 1 min after the double ageing treatment described for a Zr–15 at.% Nb alloy in Fig. 3.

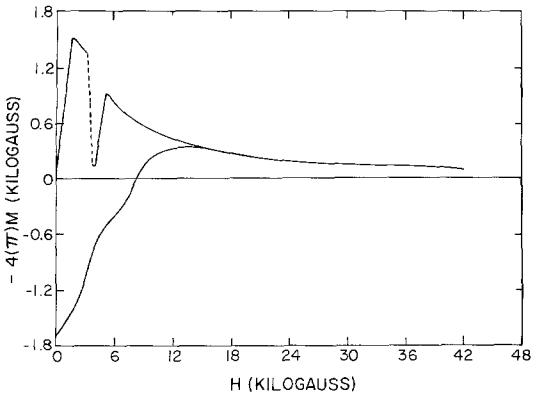

Figure 5 Effect of isothermal ageing at 350° C for 24 h on the magnetization behaviour of a Zr–15 at. % Nb alloy.

An earlier investigation [6] has shown that flux jumps occur in Zr–20 at. % Nb alloys that have been aged for periods in excess of 30 h to produce the omega phase. This behaviour is illustrated by the magnetization curves for quenched and aged Zr–20 at. % Nb alloys shown in Fig. 6. The omega

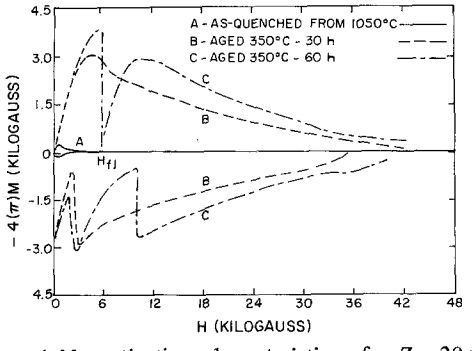

Figure 6 Magnetization characteristics of a Zr–20 at. % Nb alloy aged at 350° C.

phase formed during ageing in the 20 at. % Nb alloy can be reverted by up-quenching to 550° C [6]. The effect of this treatment on the magnetization behaviour is shown in Fig. 7, where it is seen that there are no flux jumps in this alloy after reversion and reprecipitation.

3.2. Electron microscopy and diffraction analysis

Electron microscopy and diffraction analyses were conducted in conjunction with the magnetization measurements for both the Zr–15 at. % Nb and Zr–20 at. % Nb alloys. In agreement with earlier work [4], the as-quenched Zr–15 at. % Nb alloy contained a fine distribution of athermal omega particles in a beta matrix; these particles were less than 50 Å in size. A dark-field micrograph and a selected-area diffraction pattern, Fig. 8a and b, show the microstructure obtained when the quenched alloy is aged at 225° C for 40 h. This aged alloy contains omega particles approximately 50 to 100 Å in size. When an additional ageing treatment at 350° C for 6 h is superimposed, the omega particles grow to an approximate size of 150 to 200 Å, as shown in Fig. 9a. Fig. 9b is the corresponding $\langle 1\,0\,0\rangle_\beta$ selected-area diffraction pattern showing spikes that are identified with omega reflections which do not lie exactly in the $\langle 1\,0\,0\rangle_\beta$ rel plane. If the quenched alloy is aged at 350° C for periods of 1 h and 24 h, the omega particles are approximately 250 and 450 Å as shown in Figs. 10 and 11.

It has been shown in a previous paper [6] that the beta phase is fully retained in a quenched

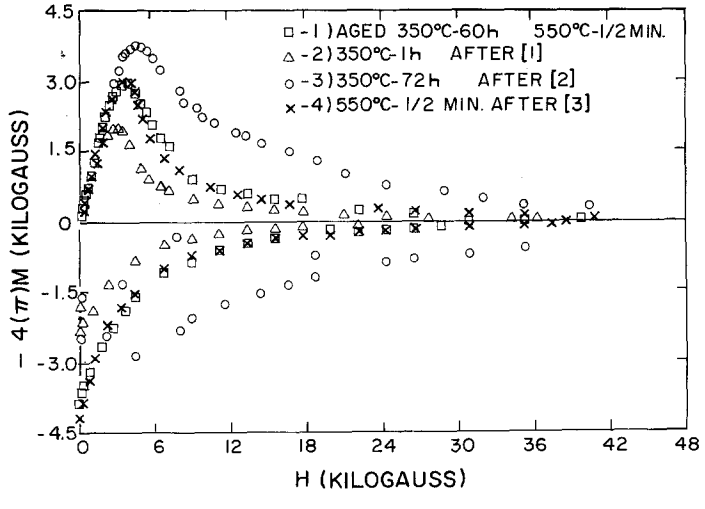

Figure 7 The effects of reversion and reprecipitation of the omega phase on the magnetization characteristics of a Zr–20 at. % Nb alloy.

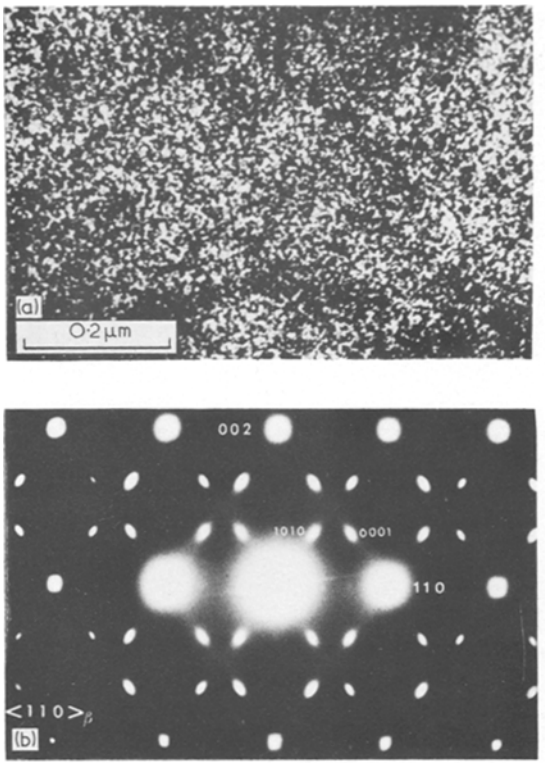

Figure 8(a) Omega particles precipitated in a Zr–15 at.% Nb alloy aged at 225° C for 40 h. Dark field obtained using a $(0\,0\,0\,1)_\omega$ reflection. (b) $\langle 1\,1\,0\rangle_\beta$ SAD pattern for the above with β and ω reflections.

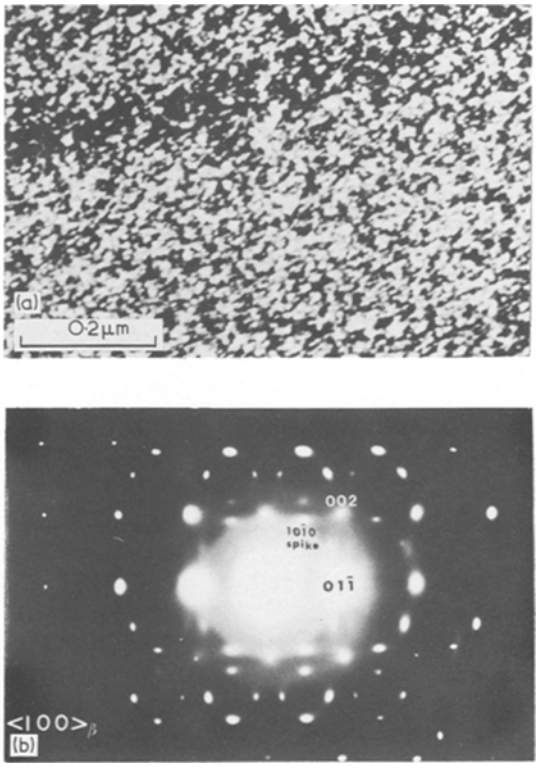

Figure 9(a) Dark-field micrograph from a $(1\,0\,1\,0)_\omega$ reflection for a Zr–15 at.% Nb alloy initially aged at 225° C for 40 h and up-quenched to 350° C and held for 6 h. (b) A $\langle 1\,0\,0\rangle_\beta$ SAD pattern for the above condition showing spikes of omega reflections that do not lie in the rel plane of the β reflection.

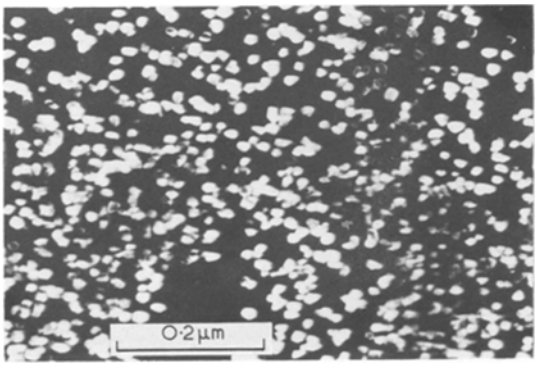

Figure 10 Isothermal omega particles imaged in the dark field using a $(0\,1\,\bar{1}\,0)_\omega$ reflection in a Zr–15 at.% Nb alloy aged at 350° C for 1 h.

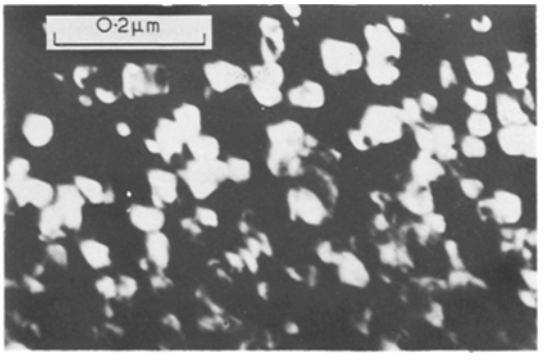

Figure 11 Well-grown omega particles in a Zr–15 at.% Nb alloy aged at 350° C for 24 h. Dark-field image from a $(0\,1\,\bar{1}\,0)$ omega reflection.

Zr–20 at.% Nb alloy and that the precipitation of the omega phase is preceded by a phase separation reaction. Fig. 12 is a bright-field micrograph of the beta lean, β_L, precipitate discs that form as a precursor to omega precipitation. The omega particles form on the β_L discs, as shown in Fig. 13, when the quenched Zr–20 at.% Nb alloy is aged at 350° C for 60 h. Complete reversion of the omega phase occurs when the aged alloy is up-quenched to 500° C for 30 sec. Subsequent ageing for 72 h reprecipitates the omega phase.

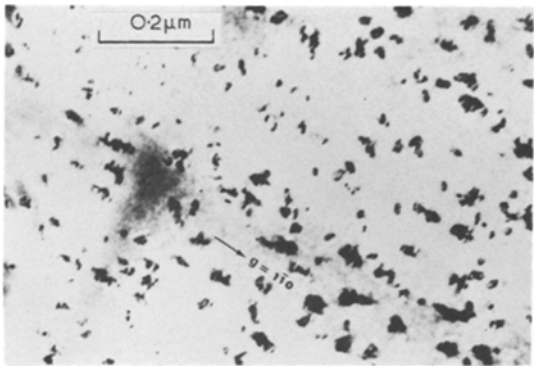

Figure 12 Coherent β_L discs observed in the bright field in a beta Zr–20 at. % Nb alloy aged at 350° C for 30 h. The line of no contrast is perpendicular to the operating reflection vector $[1\,\bar{1}\,0]_\beta$.

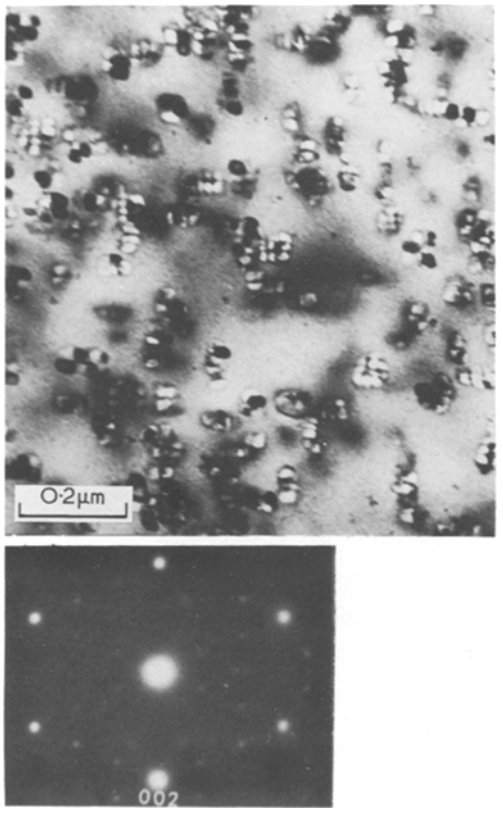

Figure 13 Colonies of cubical omega particles, precipitated on the β_L discs in a Zr–20 at. % Nb alloy aged for 60 h at 350° C. The particles are oriented in the $\langle 0\,0\,1\rangle_\beta$ directions; bright-field image for the foil orientation close to $\langle 2\,1\,0\rangle_\beta$ zone normal.

4. Discussion of results

4.1. Magnetization peak effects

For a superconductor in the mixed state the basic magnetization equation can be written in terms of the flux quantum ϕ_0 and the number of flux quanta n, per unit volume of the superconductor as follows [7]:

$$-4\pi M = H_a - n\phi_0. \tag{1}$$

For a given increase in field ΔH_a, the rate of change in the magnitude of the negative magnetization $|4\pi M|$, with respect to H_a is given by:

$$\frac{\Delta|4\pi M|}{\Delta H_a} = 1 - \frac{\phi_0 \Delta n}{\Delta H_a}. \tag{2}$$

The first peak in $|4\pi M|$ which is commonly observed in type II superconductors, arises because it is difficult to force the flux quanta into the superconductor. As the external field is increased a flux gradient is established in the surface of the superconductor to the extent of the penetration depth, and the motion of flux lines towards the interior of the specimen is opposed by the shielding currents that circulate below the surface over a distance determined by the penetration depth. When the applied field is increased by ΔH_a, the the value of $|4\pi M|$ increases and

$$\Delta n < \frac{\Delta H_a}{\phi_0}.$$

With a further increase in the applied magnetic field, the flux lines eventually overcome the opposition of the shielding currents, and the barrier to the entry of additional flux lines diminishes so that

$$\Delta n = \frac{\Delta H_a}{\phi_0}.$$

and $|4\pi M|$ reaches a maximum. The flux lines provided by ΔH_a are introduced and become pinned at the pinning sites within the superconductor.

Further motion of the flux threads towards the interior is aided by the repulsive forces from the neighbouring flux threads, and more flux lines can be introduced. Under these conditions

$$\Delta n > \frac{\Delta H_a}{\phi_0}.$$

According to Equation 2 this implies that the increment in $|4\pi M|$ is negative and $|4\pi M|$ decreases with increasing applied field. In general, beyond the maximum corresponding to the end of the Meissner region, $|4\pi M|$ decreases monotonically with an increasing applied magnetic field, H_a, and at H_{c2} approaches a value of zero. In the presence of the peak effect $|4\pi M|$ exhibits a second maximum indicative of the existence of a second barrier to the entry of flux.

4.2. Microstructural origins of the peak effect

Double peaks have been observed in the magnetization curves for a number of alloy systems, and in the case of the Ti–22.5 at. % V and Ti–20 at. % Nb alloys they have been attributed to the surface quality of the specimen [5, 8]. Baker and Sutton [9] associated the peaks in the magnetization behaviour of a quenched and aged Ti–20 at. % Nb alloy with the shielding effects of solute enriched regions around the omega particles. The existence of such solute rich regions in the form of shells around the omega particles in Ti–Nb alloys was established by Hatt and Rivlin [10], based on single crystal X-ray diffraction intensity profile analysis. Karasik *et al.* [11] have attributed a peak effect in a Ti–22 at. % Nb alloy to the transition of the omega particles from the superconducting to the normal state at low applied magnetic fields. Kramer and Rhodes [12] and Koch and Carpenter [13] suggested that when the precipitate spacing approaches the fluxoid spacing the flux pinning should be most effective, thereby leading to a peak value for the pinning force.

In the present investigation, the peaks in the magnetization curves occur at magnetic fields ranging from 6 to 10 kG as shown in Fig. 1 to 3. The magnitude and position of the peaks depend on the thermal treatment, especially as it relates to the formation of the omega phase.

The flux line spacing for a triangular flux line lattice can be calculated from the relationship [3]:

$$d_f = \left[\frac{1.15\phi_0}{B_e}\right]^{\frac{1}{2}} \qquad (3)$$

where ϕ_0 equals 2×10^{-7}G-cm^2, and B_e can be approximated by the magnitude of the applied field, H_a [3], since $H_a \gg M$. The calculated lattice spacing, d_f, based on the value of H_a at the magnetization peak, ranges from 350 to 450 Å, which is 3 to 4 times larger than either the size or spacing of the omega particles shown in Figs. 9a and 10. This size relationship cannot account for the peak effect on the basis of the matching theory proposed by Kramer and Rhodes [12] and Koch and Carpenter [13].

4.3. Flux pinning model for Zr–Nb alloys

In a Zr–15 at. % Nb alloy aged for 40 h at 225° C the omega particles range in size from 60 to 100 Å which is less than the estimated coherence length of 120 Å. Under these conditions the omega particles have a negligible influence on the pinning of the flux lines, and a second peak in the magnetization curve does not arise. If the ageing treatment is continued for 6 h and the ageing temperature is increased to 350° C, the omega particles grow to a size of approximately 150 to 200 Å, while the coherence length of the alloy rises to approximately 140 Å. A second peak in the magnetization curve is clearly evident, as shown in Fig. 3. The peak effect is, therefore, sensitive to the size and volume fraction of the omega phase, consistent with the conditions dictated by the effect of the coherence length. The elimination of the omega phase structure by a reversion treatment leaves solute lean beta zones surrounded by an enriched ring. Under these conditions a peak effect is not observed, leading to the conclusion that the solute enriched ring is not a significant factor contributing to the peak effect. The continued formation of the omega phase during ageing increases the size and volume fraction of the omega particles, and under these conditions no peak effect is observed, but a flux jump occurs at an applied field of approximately 4 kG as shown in Fig. 5.

Karasik *et al.* [11] state that when the size of the omega particles is comparable in magnitude to the coherence length, the matrix induces superconducting behaviour in them at temperatures less than the value of T_c for the matrix. The average size of the omega particles in the aged Zr–15 at. % Nb alloys that exhibit the peak effect is of the order of the coherence length, so that at 4.2 K the omega particles would be superconducting in the absence of an applied magnetic field. The omega particles in a Zr–Nb alloy which for the bulk value of T_c is between 6.2 and 6.8 K are, therefore, expected to undergo a transition from the superconducting to the normal state as the applied field is increased. In these alloys when the applied field overcomes the Meissner effect, the flux lines penetrate the specimen leading to a decrease in the value of $|4\pi M|$. When a minimum occurs in the magnetization curve, it indicates that the omega particles which were superconducting at zero external field have become normal and saturated with flux. Once the saturation condition is achieved, the flux lines trapped by the omega particles impede the introduction of additional flux. Such a barrier to the entry of flux accounts for the second peak observed in Figs. 2 and 3. The capability of the alloy to resist the entrance of additional flux therefore depends upon the volume fraction, the

particle size, and the interparticle spacing of the omega phase. It can be seen from Figs. 2 and 3 that increasing the ageing time increases the peak height from 0.45 to 0.74 kG, and the applied field at which the peak occurs is decreased from approximately to 10 kG to 6 kG. A further increase in the ageing time doubles the dimagnetic susceptibility and a pronounced instability in the form of a flux jump occurs at 4 kG. An examination of the corresponding photomicrographs shows that if the omega particle size is less than 100 Å, there is no effect on the magnetization, while an increase in particle size from 100 Å to 200 Å promotes the peak effect. When the particle size has reached approximately 450 Å, and the volume fraction of the omega phase is sufficiently large the transition to the normal state eliminates bulk diamagnetic behaviour, and the alloy exhibits a flux jump. Following the flux jump, the specimen again exhibits bulk superconductivity that is determined by the influence of the matrix phase in which the omega particles now act as normal pinning sites.

Flux instabilities are characterized by an instantaneous decrease in the diamagnetic susceptibility, and near H_{c1} such instabilities can be severe enough to result in almost zero magnetization [14]. The source of these flux jumps is attributed to the collective dissipative motion of flux bundles in the superconductor [15], and the origin of such a disturbance may be either mechanical or thermal. The resulting motion of the bundle in the flux density gradient, when it occurs in a short period of time, leads to localized heating above the ambient temperature. This effect can be sufficient to unpin more flux lines, thereby resulting in a cascade process of collective flux motion. Under adiabatic conditions the heating effect may cause the local temperature to exceed the value of T_c [16]. In an alloy containing weak superconducting precipitates with a size approaching the coherence length there would be enhanced pinning when the precipitates are converted to the normal state [1–3]. If the volume fraction of the precipitate is great enough, conversion to the normal state is expected to eliminate the bulk superconducting behaviour of the material, and the avalanche of flux lines would be manifested as a flux jump.

The dependency of the peak effect on the presence of the omega phase is substantiated by comparing the magnetization curves for the 15 at.% Nb alloy with those for the Zr–20 at.% Nb alloy. The formation of solute lean zones precedes the initiation of omega precipitation in the 20 at.% Nb alloy which contains no athermal omega phase after quenching to room temperature [6]. After 30 h ageing, there is no definite evidence of omega precipitation in either the electron micrographs or the selected-area electron diffraction patterns taken at room temperature. However, a slight peak effect is evident beyond the initial maximum in the magnetization curve as shown in curve B, Fig. 6 for a Zr–20 at.% Nb alloy aged 30 h at 350° C. This anomaly is interpreted as a manifestation of small quantities of the omega phase, formed either during ageing or by the athermal transformation associated with the solute lean zones on cooling to 4.2 K. After 60 h ageing at 350° C, the presence of the omega phase is clearly evident at the interfaces of the solute lean zones with an average particle size of about 200 Å as shown in Fig. 13. the magnetization curve exhibits enhanced diamagnetic susceptibility and a flux jump at approximately 5 kG, corresponding to a flux line spacing of approximately 630 Å. This spacing approximates the size of multi-variant groupings of particles of the omega phase formed after 60 h at 350° C. Such a size relationship is an optimum condition for pinning with one flux quantum per omega cluster.

Since reversion of the omega phase eliminates both forms of instability, re-ageing should optimize the pinning efficiency of the omega phase in conjunction with the solute enriched matrix. The effectiveness of re-ageing after reversion has been demonstrated for a Zr–20 at.% Nb alloy where both H_{c2} and the magnetic hysteresis were increased over the quenched and aged condition as shown in Fig. 7.

Reversion of the omega phase eliminates the flux jump phenomenon since the magnetization behaviour is then controlled by the solute modulations that remain in the matrix. Re-ageing the alloy requires the re-nucleation of omega in conjunction with these modulations. The subsequent magnetic stability of the alloy depends on the combined effect of the solute modulations and the omega precipitate. In a 20 at.% Nb alloy aged at 350° C for times in excess of 30 h the magnetization behaviour reflects the presence of the omega phase, and flux jumps occur. In the reverted alloy solute modulations are already well established, and the subsequent precipitation of the omega phase requires a considerable ageing period before the solute modulations are consumed to a sufficient degree for the omega phase to have a pre-

dominant effect on the magnetic behaviour. When the re-aged alloy is reverted a second time, the magnetic behaviour is identical with that exhibited after the first reversion, indicating that the solute modulations in the matrix are reproducible prior to any alpha precipitation.

5. Conclusions

(1) A "peak effect" has been observed in Zr–Nb alloys, and it is sensitive to both the size and volume fraction of the isothermal omega phase.

(2) The "peak effect" is removed by a reversion treatment that eliminates the omega phase structure.

(3) The occurrence of the "peak effect" is explained on the basis of a second barrier to the entry of flux, presented by the omega particles that undergo a superconducting to normal transition as the applied magnetic field is increased.

(4) An instability in the magnetic behaviour in the form of a flux jump occurs when the omega particles are large and their volume fraction great enough so that their transition to the normal state suppresses the bulk diamagnetic behaviour.

(5) The reversion of the omega phase eliminates the flux jump phenomenon, and the subsequent magnetic behaviour is a function of the remnant solute modulations. When the omega phase is re-nucleated and grown to a size that exceeds the coherence length of the alloy, the magnetic irreversibility and stability are significantly enhanced, and the flux jump phenomenon does not reappear.

Acknowledgement

The work reported in this paper is part of a programme supported by the Energy Research and Development Administration, Contract AT(45-1)-2225-T13).

References

1. J. D. LIVINGSTON and H. W. SCHADLER, *Prog. Mat. Sci.* **12**((1964).
2. D. DEW HUGHES, *Mater. Sci. Eng.* **1** (1966) 2.
3. *Idem, Rep. Prog. Phys.* **34**,(1971) 821.
4. S. L. NARASIMHAN, R. TAGGART and D. H. POLONIS, *J. Nucl. Mater.* **43** (1972) 258.
5. T. S. LUHMAN, R. TAGGART and D. H. POLONIS, *Scripta Met.* **6** (1972) 1055.
6. S. L. NARASIMHAN, R. TAGGART and D. H. POLONIS, *Scripta Met.* **7** (1973) 1089.
7. D. ST. JAMES, G. SARMA and J. R. MOON, "Type II Superconductivity" (Pergamon Press, 1971).
8. R. R. HAKE, *Phys. Rev.* **158** (1967) 368.
9. C. BAKER and J. SUTTON, *Phil. Mag.* **19** (1969) 1223.
10. B. A. HATT and V. G. RIVLIN, *J. Phys. D.* **1** (1968) 1145.
11. V. R. KARASIK, N. G. VASIL'EV, and V. G. ERSHOV, *Sov. Phys. JETP*, **32** (1971) 433.
12. D. KRAMER and C. G. RHODES, *Trans. Met. Soc. AIME* **239** (1967) 1612.
13. C. C. KOCH and R. W. CARPENTER, *Phil. Mag.* **25** (1972) 303.
14. S. H. GEODEMOED, C. VAN KOLMESCHATE, J. W. METSELOAR and D. DE KLERK, *Physica* **31** (1965) 573.
15. Y. B. KIM, C. F. HEMPSTEAD and A. R. STRNAD, *Phys. Rev. Letters* **9** (1962) 306.
16. S. L. WIPF, *Phys. Rev.* **161** (1967) 404.

Received 29 November 1974 and accepted 11 June 1975.